EurJIC
European Journal of Inorganic Chemistry

A Journal of ChemPubSoc Europe

Accepted Article

Title: An insight into the metal content-structure-property relationship in lanthanide metal-organic frameworks: optical studies, magnetism and catalytic performance

Authors: Germán Ernesto Gomez, Elena Virginia Brusau, Joaquín Sacanell, Galo Soler-Illia, and Griselda Edith Narda

To be cited as: *Eur. J. Inorg. Chem.* 10.1002/ejic.201701474

Link to VoR: http://dx.doi.org/10.1002/ejic.201701474

WILEY-VCH

An insight into the metal content-structure-property relationship in lanthanide metal-organic frameworks: optical studies, magnetism and catalytic performance

Germán E. Gomez*[a], Elena V. Brusau[a], Joaquín Sacanell[b], Galo J. A. A. Soler Illia[c], Griselda E. Narda*[a]

Abstract: Two series of metal–organic frameworks (MOFs) based on a flexible ligand and trivalent lanthanides were obtained hydrothermally in order to explore their optical properties at low temperatures, magnetism and catalytic activity in relation to their structural features. A multisite analysis was performed according to the 4f-4f transitions. Moreover, the heterogeneous catalytic activity of the series was evaluated in one-pot cyanosilylation with benzaldehyde as substrate. Recyclability, structure conservation and catalytic efficiency were also evaluated and compared with analogous compounds.

Introduction

During the last decades, the Metal Organic Frameworks (MOF) have been the focus of interest because of their potential applications in catalysis,[1] ion exchange and chemical separation,[2] drug delivery,[3] luminescence[4] and magnetism[5] converting them into promising multifunctional materials for emerging devices[6]. Particularly, this study has been addressed to the synthesis of new MOFs architectures with mechanical,[7,8] optical,[9] catalytic,[10,11,12] thermo,[10,13] chemical[7,14] sensing and magnetic[15] or antibacterial[8] properties, exploring their *structure-property relationships*. Specifically, the synthesis and structural characterization of flexible ligand-based coordination polymers with multifunctional properties is an important issue in our research group. Scheme 1 exhibits the pathways for designing new MOFs materials.
Regarding the linkers, polycarboxylic aliphatic ones are considered as appropriate building blocks because of their flexibility along with their versatile coordination ability that offer many possibilities for constructing frameworks with unique architectures and useful properties[16].

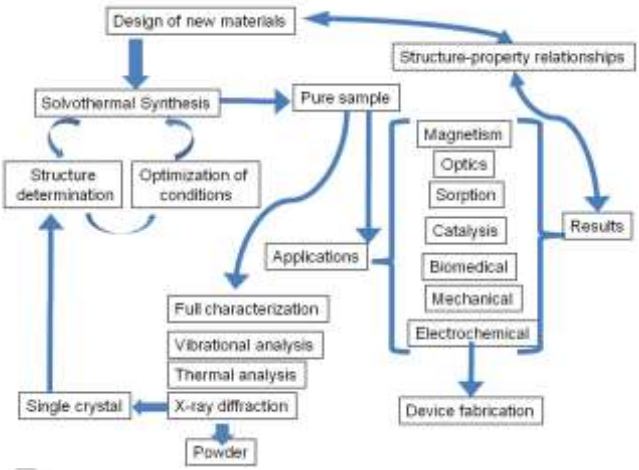

Scheme 1: General pathways of the procedure for the design of new MOFs materials.

In this sense, the succinate ligand is a flexible dicarboxylate anion that has been employed not only in the synthesis of transition metal-based frameworks[17] but also in those with lanthanides[18] and actinides[19] ones allowing the development of a great number of new structures. Besides, lanthanide-succinate MOFs were reported as heterogeneous catalysts[20] for the reduction of nitroaromatic compounds. On the matter, we have previously obtained several lanthanide-succinate frameworks with magnetic[21] and catalytic properties.[22] Moreover, the non-centrosymmetric 2,2-dimethylsuccinate (2,2-dms) as ligand has also been explored by us obtaining laminar Er-MOFs whose formation was governed by kinetic or thermodynamic control.[11b] In addition, several MOFs based on Y(III) or lanthanides and 2,2-dms or 2,3-dimethylsuccinate (2,3-dms) were reported as potential solid emitters upon UV excitation.[23] With the aim to extend our studies on lanthanide-succinate MOFs, the use of 2,3-dms, 2-methylsuccinate and 2-phenylsuccinate ligands has been investigated to assess the impact of the conformational flexibility of the aliphatic subunits along with the coordination geometry

[a] Instituto de Investigaciones en Tecnología Química (INTEQUI). Área de Química General e Inorgánica "Dr. G. F. Puelles", Facultad de Química, Bioquímica y Farmacia, Chacabuco y Pedernera, Universidad Nacional de San Luis, 5700 San Luis, Argentina. E-mails: gegomez@unsl.edu.ar and gnarda@unsl.edu.ar
[b] Departamento de Física de la Materia Condensada, Gerencia de Investigación y Aplicaciones, Comisión Nacional de Energía Atómica (CNEA), San Martín, Buenos Aires, Argentina.
[c] Instituto de Nanosistemas. Universidad Nacional de San Martín. Av. 25 de Mayo 1021, San Martín, Buenos Aires, Argentina.
Supporting Information (SI) available: [powder XRD patterns and graphics]. See DOI: 10.1039/x0xx00000x

preferences on the development frameworks. A set of dense Ln-MOFs obtained by us and their corresponding structural and topologic features is shown in Figure 1: **Ln-dms-1**[9a] (Ln=Nd, Pr, Sm, Eu), **Ln-dms-2**[9a] (Ln=Tb, Dy, Ho, Er, Yb) (dms=2,3-dimethylsuccinate), **Ln-psa**[9b,10] (Ln=Nd, Pr, Eu, Sm, Gd, EuTb, EuGd) (psa=2-phenylsuccinate) and **Ln-msuc**[14a] (Ln=Nd, Dy, Eu, Gd, Tb) (msuc=2-methylsuccinate).

The design of MOFs for preparing active and selective catalysts obeys to the possibility of achieving outstanding textural properties and high metal contents.

Thus, several Ln-MOFs were successfully tested as heterogeneous catalysts for hydrodesulfurization of thiophene[22, 24] and oxidation of methylphenylsulfide[25] reactions.

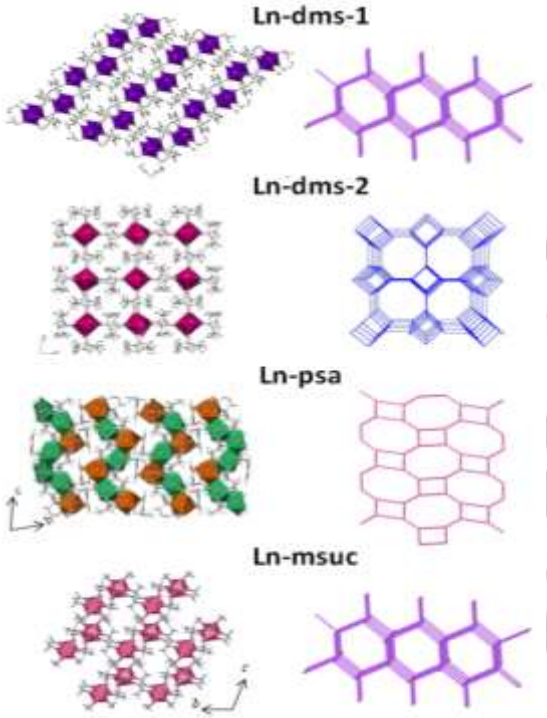

Figure 1: Structures and topologies of Ln-MOFs taken from References 9a, 9b and 14a.

Nevertheless, the relatively limited chemical and thermal stability of MOFs, along with the presence of metallic sites blocked by the organic spacers, have somehow restricted their use in this area. To overcome these drawbacks, new synthesis strategies have been applied in the last years. In order to demonstrate Lewis acid properties in MOFs, the cyanosilylation of aldehydes and ketones (Cyanosilylation Reactions, CSRs) are commonly tested[1]. In this context, Trimethylsilyl cyanide (TMSCN) is one of the most useful cyanating reactants for nucleophilic addition to carbonyl compounds to obtain cyanohydrin trimethylsilyl ethers, which are important intermediaries in organic synthesis of new building blocks.[26] For this reason, the development of efficient and selective catalysts for CSRs is relevant in heterogeneous catalysis.[27]

On the other hand, the spectroscopic properties of lanthanide ions are attractive since their [Xe]$4f^n$ electronic configuration generates a variety of electronic levels (see Figure S1).

Besides, the optical studies of materials containing lanthanide ions could be grouped in one (or more) of the following studies[28]: optical absorption (a), emission (b), determination of radiative and non-radiative rate constants (k_{rad} and k_{nr}) (c), quantum yields (d), determination of Judd-Ofelt parameters ($\Omega_{2,4,6}$) (e) and the corresponding description about the different energy processes between the lanthanides ions and their surroundings (f). When lanthanide ions are under the influence of the crystal field (CF) of the surrounding ligands it is assumed that $^{2S+1}L_J$ levels are split depending on the local symmetry. When the CF is stronger, several levels can be admixed.

The optical properties of lanthanide based-inorganic materials[29,30,31] suppose a continuous research focus in terms of fundamental knowledge but also for potential photonic applications[32,33,34,35]. In addition, temperature and chemical sensing is a field in constant growing in which Ln-MOFs have been reaching more participation [36]. Particularly, for laser applications [37] the study of the spectroscopic parameters derived from the CF analysis by the high resolution absorption spectra (HRAS) and photoluminescence is required. The absorption and emission spectra of lanthanide-compounds into the visible, UV and NIR regions are attributed to 4f-4f transitions; they exhibit fine lines with oscillator strength constants around 10^{-6}.

In this work, we present a detailed description of HRAS for **Ln-dms-1** and **Ln-dms-2** compounds as well as an in-depth study of the optical properties derived from the 4f-4f transitions in relation with the structural features. Moreover, the magnetic properties of the series were also studied in terms of magnetic susceptibility as a function of

temperature into the 50-300 K range. Finally, the catalytic performance of these compounds was examined by selecting some members of the **Ln-dms-1** and **Ln-dms-2** sets in the CSR with the aim to identify the role that Lewis metal sites play in the carbonyl activation mechanism. Moreover, green chemistry metrics were employed to evaluate the efficiency of the catalytic process.

Structural description

According to the crystallographic data[9a], under identical synthesis conditions, two families of compounds were obtained: one belonging to the triclinic space group Pī with formula $[Ln_2(2,3\text{-dms})_3(H_2O)_2]$ (Ln=Nd-Eu) (**Ln-dms-1**); the other set crystallizes in the tetragonal space group $P4_32_12$ $[Ln_2(2,3\text{-dms})_3]$ (Ln=Tb-Yb) (**Ln-dms-2**). There are two crystallographically non-equivalent lanthanide atoms in **Ln-dms-1** Primary Building Unit (PBU). Both of them are surrounded by eight oxygen atoms belonging to carboxylate groups and another one coming from one coordinated water molecule; meanwhile, **Ln-dms-2** compounds exhibit three non-equivalent lanthanide ions in octa-coordinated environments, all of them belonging to the carboxylate linkers (Figure 2). The Secondary Building Units (SBUs) in both compounds is consisting with polyhedra chains. Besides, **Ln-dms-1** and **Ln-dms-2** present a microporous nature exhibiting one-dimensional channels along the *a* direction with void volumes of 114.4 $Å^3$ and 892.6 $Å^3$, respectively. The different porous geometry and metallic content make these compounds suitable for exploring their catalytic performance and optical properties.

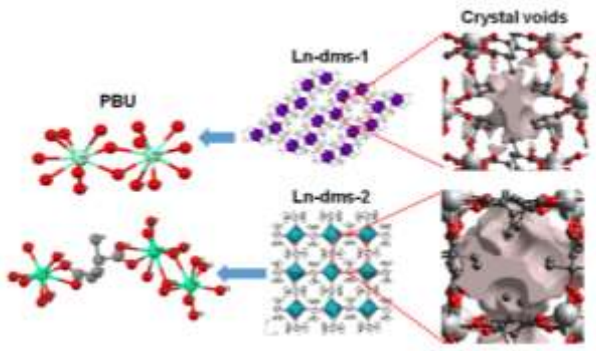

Figure 2: PBUs, SBU development and Crystal void representations for **Ln-dms-1** and **Ln-dms-2**.

Optical and magnetic properties

Optical studies

As can be seen in Figure 3, the spectrum of **Pr-dms** presents lines into the visible and IR regions ascribed to 4f-4f transitions belonging to Pr^{3+} ion's 4f shell, which can be deduced from the absorption and the diffuse reflectance spectra at room temperature (Figure S2). The lines are associated to the depopulation of the $^3H_4$ level to $^3P_2$ (444 nm), $^3P_1$ (469 nm), $^3P_0$ (482 nm) and $^1D_2$ (barycenter localized at 591 nm) excited levels; being $^3H_4$ the fundamental electronic level of the $4f^2$ configuration. The $^3H_4 \rightarrow {}^3P_2$ transition is dominant in intensity due to its *hypersensitive character*. The intensities of the $^3H_4 \rightarrow {}^3P_0$ and $^3H_4 \rightarrow {}^3P_1$ transitions can be explained by the mechanism of *polarization dynamic coupling* (induced radiation by ligand polarization).[38] The HRAS shows well-structured bands in which the different "Stark" components can be observed (see Figure 3).

It is expected that a $^{2S+1}L_J$ transition should be split into 2J+1 components when n-lanthanide sites are present into the crystalline structure. The presence of two signals for the $^3H_4 \rightarrow {}^3P_0$ at low temperature suggests a local environment composed by two independent Pr^{3+} ions. Besides, the energy position of the $^3P_0$ level located at 20716 cm^{-1} into the barycenter curve,[39] is comparable with the reported values of inorganic compounds with praseodymium in a nona-coordinated environment (see Figure S3 and S4). The barycenter curves relate the energy values of the $^3H_4 \rightarrow {}^3P_1$ transition with to the $^3H_4 \rightarrow {}^3P_0$ one, or the energy difference (ΔE) between the $^3H_4 \rightarrow {}^3P_0$ and $^3H_4 \rightarrow {}^1D_2$ transitions with respect to $^3H_4 \rightarrow {}^3P_0$ one. A similar procedure was performed by Antic-Fidancev et al. for a Pr-glutarate, the CF studies by HRAS being useful to support the structural characterization.[39]

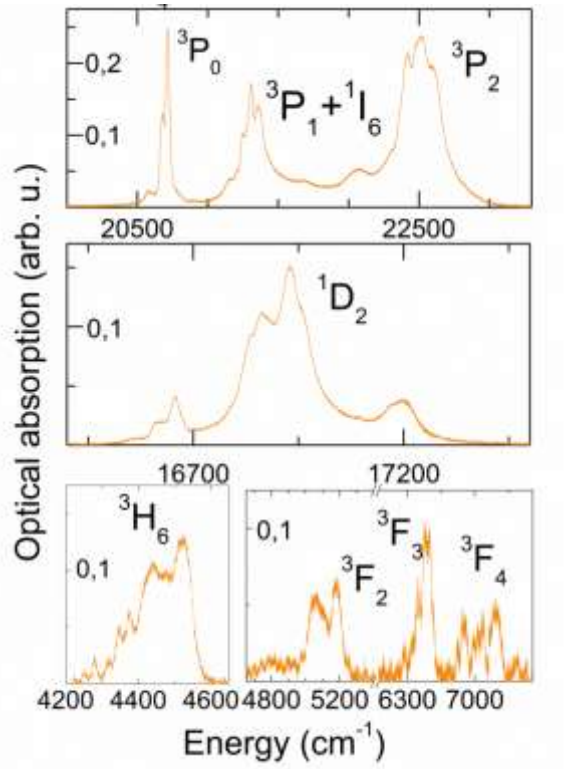

Figure 3: HRAS at 6 K of **Pr-dms** showing the principal 4f transitions from $^3H_4$ level into the visible and infrared regions.

The optical study of Nd-materials is relevant for lasers design, the Nd:YAG (YAG=$Y_3Al_5O_{12}$) being the most referenced in optoelectronics. In the case of **Nd-dms**, the spectra at 6 K show structured bands into the UV to NIR region, as can be seen in Figure 4. All transitions start from the $^4I_{9/2}$ fundamental electronic level to different excited states. The presence of two bands ascribed to the hypersensitive $^4I_{9/2}\rightarrow{}^2P_{1/2}$ transition suggests the existence of two active neodymium centers, in coincidence with the crystallographic information.[9a] This fact is also supported by the thermal evolution of the mentioned transition when the temperature increases from 25 to 150 K. As can be seen in Figure S5 the intensity of the multiplet located at 429 nm decreases 41% when temperature reaches 150 K, meanwhile the corresponding one at 430.5 nm, increases 43%.

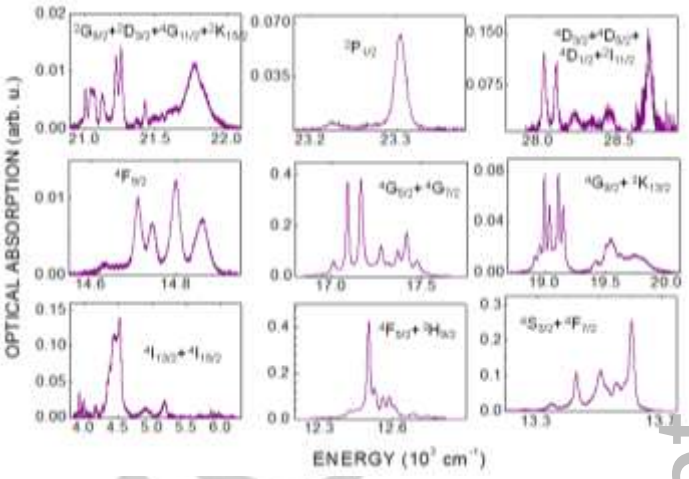

Figure 4: HRAS of **Nd-dms** recorded at 6 K from the NIR to UV regions.

The $4f^5$ configuration of Sm^{3+} is characterized by 198 transitions that can be split into 1001 energy levels; so, its energetic scheme is one of the most complex among those of the trivalent lanthanide ions.

The HRAS of **Sm-dms** was measured into the UV-Vis-NIR regions (350-1850 nm) corresponding to the transition from the $^6H_{5/2}$ level to the up-level excited states (see Figure 5). The signals in the NIR region assigned to the $^6H_{13/2}$ and $^6F_{5/2\text{-}11/2}$ transitions can be observed as well-structured bands. Figure S6 shows the coincidence of the 4f-4f transitions in the absorption and reflectance spectra measured at RT.

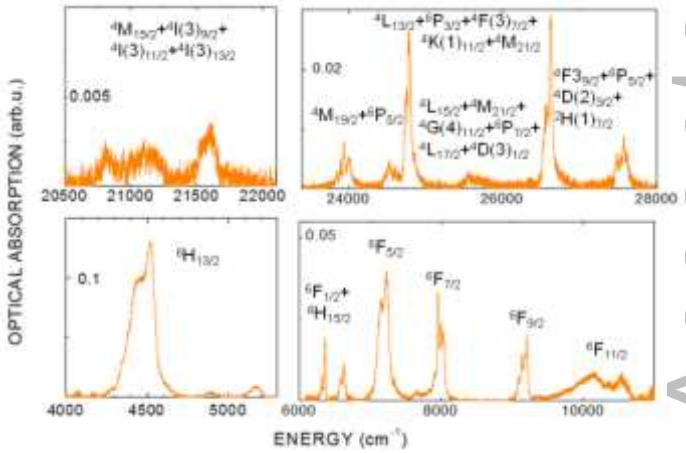

Figure 5: HRAS of **Sm-dms** recorded at 6 K from the NIR to UV regions.

The energy levels assignment of the $4f^{10}$ configuration of Ho^{3+} is usually complicated and poor information is found in MOF literature. The HRAS of **Ho-dms** collected at 6 K into the 360-2000 nm range (Figure 6), allowed the

identification of transitions originated in the $^5I_7$ energy level.

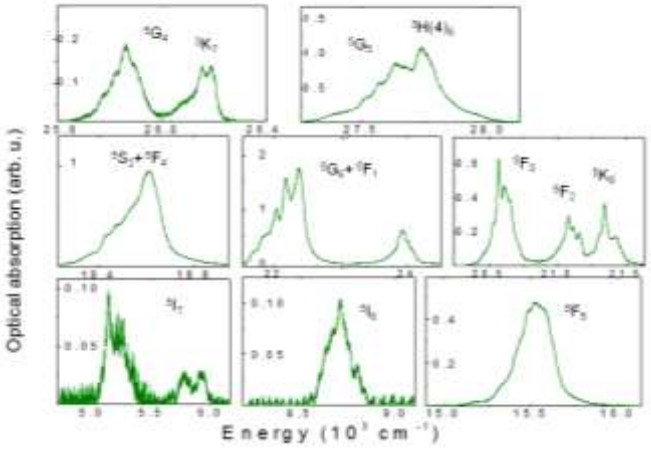

Figure 6: HRAS of **Ho-dms** recorded at 6 K from the NIR to UV regions.

The CF analysis of the HRAS of **Er-dms** shows a coexistence of various Er^{3+} centers. The study at low temperature of the Er^{3+} $4f^{11}$ configuration leads to the identification of the characteristic bands from the $^5D_{5/2}$ fundamental state into the 250-1660 nm range (Figure 7). At 6 K, the transitions from the $^5I_{15/2}(0)$ were identified and resolved, even the weaker $^4I_{11/2}$, $^4F_{7/2}$ and $^4F_{3/2}$ ones. The RT measurements (reflectance and absorption) also fit well (Figure S6). HRAS of **Yb-dms**, shows the triplets corresponding to the $^2F_{7/2} \rightarrow {}^2F_{5/2}$ transition (Figure 8). The multiplet nature of this signal is also a strong evidence of different ytterbium sites.

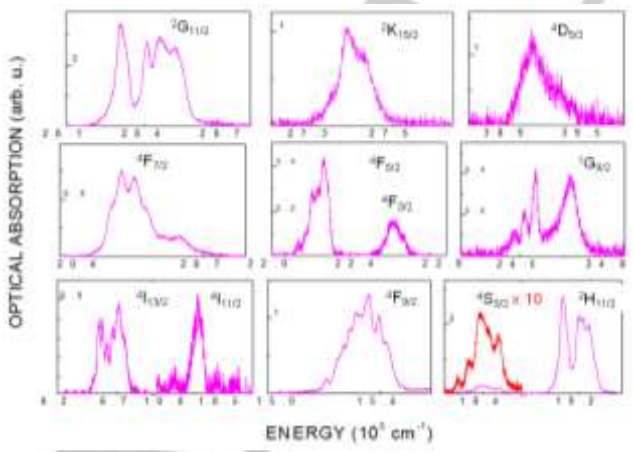

Figure 7: HRAS of **Er-dms** recorded at 6 K from the NIR to UV region.

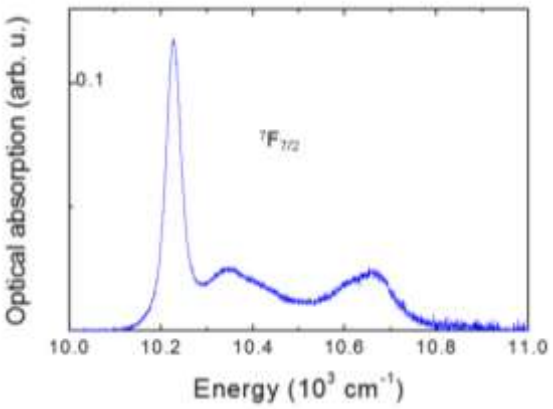

Figure 8: HRAS of **Yb-dms**.

Magnetic properties

The behaviour of the materials under a magnetic field is important for solid characterization; particularly, the magnetic properties at variable temperature allow the study of phase transitions usually associated to structural ones. The temperature dependence of the magnetic susceptibility is presented as $\chi_M \cdot T$ and χ_M^{-1}. All data are presented per mol of **Nd-dms**, **Tb-dms**, **Dy-dms**, **Ho-dms** and **Er-dms**, respectively (Figure 9). All samples present a paramagnetic behaviour following the Curie-Weiss law; $\chi_M \sim C/(T-\theta_{CW})$. For most of the compounds, θ_{CW} is close to zero, with the exception of **Nd-dms** for which a $\theta_{CW} \sim -36$ K, was obtained, suggesting a low temperature antiferromagnetic interaction.

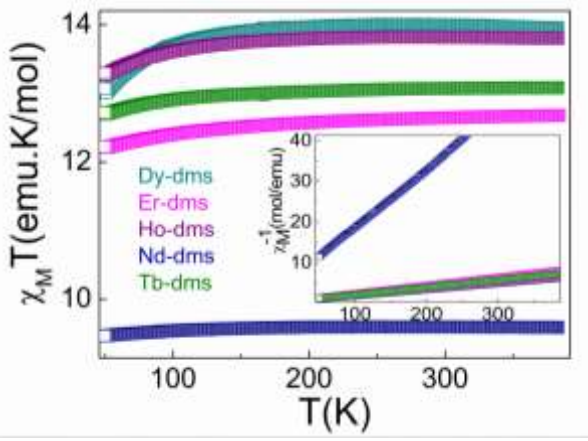

Figure 9: Temperature dependence of $\chi_M \cdot T$ and χ_M^{-1} (inset) for **Ln-dms-1** (Nd) and **Ln-dms-2** (Dy, Tb, Ho and Tb) compounds measured into the 50-300 K range under the application of a magnetic field of 1 Tesla.

Table 1 presents the values of χ_M.T at 300 K for all compounds, obtained from the magnetization data which was compared with the corresponding values from the isolated trivalent ions.[40] In most of the cases, the magnetic susceptibility data is in agreement with that corresponding to the isolated ions at the ground state. For **Nd-dms**, a significant difference of around 13% can be observed, which also suggests a low temperature antiferromagnetic interaction between Nd ions as was previously reported for related coordination polymers.[14a]

Table 1: χ_M.T values for **Ln-dms-1** (Nd) and **Ln-dms-2** (Dy, Tb, Ho and Tb) compounds in comparison with free lanthanide ions (first column).

Ln-dms	χ_M·T(300 K) (emu.K/mol) from Ref. 40	χ_M·T(300 K) (emu.K/mol) this work	f^n	ground state
Nd-dms	1.64	1.45	f^3	$^4I_{9/2}$
Tb-dms	11.82	11.75	f^8	$^7F_6$
Dy-dms	14.17	14.07	f^9	$^6H_{15/2}$
Ho-dms	14.07	13.97	f^{10}	$^4I_8$
Er-dms	11.48	10.62	f^{11}	$^4I_{15/2}$

Catalytic studies

According to Corma et al.,[1] the most employed strategies for designing catalytic MOFs are: a) Obtaining MOFs with Coordinatively Unsaturated Metal Sites (CUMs) and b) Post-synthesis Modification (PSM).

Continuing with our study about the exploration of the catalytic behaviour of Ln-MOFs, here we report the performance in CSRs of the **Ln-dms-1** and **Ln-dms-2** families. CSRs are important C-C bond-forming reactions catalyzed by Lewis acids/bases. MOFs are selected as heterogeneous catalysts for Lewis acid reactions type because of their particular reactivity and selectivity under mild conditions.[41,42] The catalytic activity of these compounds is evaluated under soft conditions and low catalyst charge. Besides, a comparison with results previously reported for **Ln-psa**[10] was performed.

The following **Ln-dms** compounds, used without pre-activation, were tested: **Nd-dms**, **Sm-dms**, **Eu-dms** (**Ln-dms-1**), **Ho-dms**, **Er-dms**, and **Yb-dms** (**Ln-dms-2**) Cyanosilylation of benzaldehyde was carried out using TMSCN, under the following conditions: room temperature, inert N_2 atmosphere, and 5 mmol% of catalyst. The final product resulted in 2-phenyl-2-(trimethylsilyl) acetonitrile (Scheme 2).

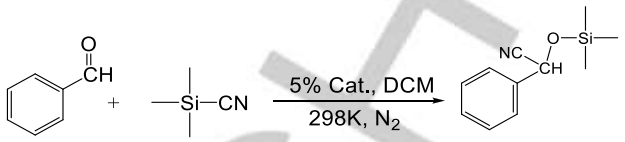

Scheme 2: CSR of benzaldehyde employing TMSCN.

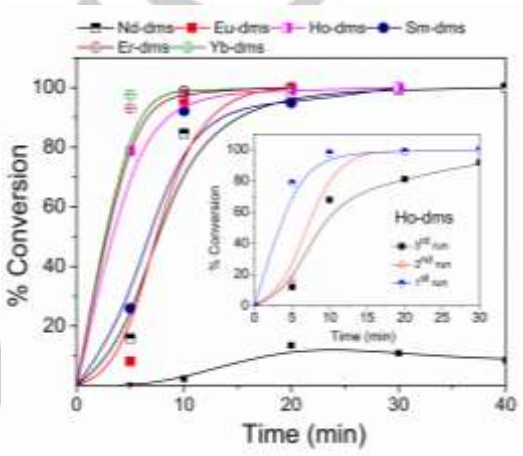

Figure 10: Kinetic profiles of CSR with **Ln-dms-1** and **Ln-dms-2** compounds as catalysts. The black curve shows the kinetic profile of the reaction system without catalyst. Inset: Kinetic profile in three consecutive reaction cycles employing **Ho-dms** as catalyst.

As it was previously described, the structural elucidation determined two coordinated water molecules per two nonequivalent nona-coordinated lanthanide atoms in **Ln-dms-1** (see PBU in Figure 2), meanwhile in **Ln-dms-2**, the metal centers are located in an octa-coordinated surrounding without water molecules. This fact leads to different catalytic performances. In this sense, the lower the coordination number, the higher the possibility of substrate-catalyst interaction. In addition, **Ln-dms-2** compounds exhibit a higher void volume in relation with **Ln-dms-1** ones (Figure 2), allowing a higher substrate-catalyst contact.

As is it well-known, lanthanides have Lewis acid strength, which is closely related to the ionic radii. In some cases, reactions that involve acid catalysis are well-defined because the reactivity increases

along with the *lanthanide contraction*. **Ln-dms-2** set presents the highest activity with a Turn Over Frequency[43] (TOF) ranging between 189.1-237 h^{-1} which is in accordance with the increase of the metal acidity towards Yb. As it was seen in similar frameworks,[11,12] the reaction is ruled by the Lewis acid character of the catalyst.

Moreover, if the catalytic performance of **Ln-dms-1** family is compared with those of the **Ln-psa** one, (see Table 2) higher TOFs and yields are achieved in short periods. This behaviour can be explained in terms of the steric effect given by the phenyl groups, which is detrimental for substrate interaction.

According to these results, it can be plausible to propose that the reaction mechanism takes place *via activation of the carbonyl by unsaturated metallic centers* (Figure 12).

Regarding the detrimental effect of water content in the luminescence behavior of **Eu-dms** that was previously reported by us,[9a] this effect was also evaluated in relation to the catalytic performance for anhydrous **Nd-dms** (**Nd'-dms**). Crystallinity conservation of **Nd-dms** upon dehydration was confirmed previously to be employed as catalyst in CSR (Figure S9). Water removal generates a CUM site per metal center and as it can be seen in Figure 11, the TOF value increases as well as the total conversion is reached. Thus, the catalytic behavior of the **Nd'-dms** resembles that of the **Ln-dms 2**. In summary, the combination of factors such as metal acidity, higher void volume and lower coordination number, allows **Ln-dms-2** series to exhibit a better catalytic performance.

Recycling Test. In order to study the possible recyclability, **Ho-dms** was selected and reused under the same conditions during three consecutive cycles (Figure 10). X-ray diffraction patterns obtained before and after the recycling tests did not show significant changes, thus confirming the structure of **Ho-dms** is retained (Figure S8). The activity, structure and crystallinity were unaltered after the reactions, demonstrating the heterogeneous nature of the catalyst.

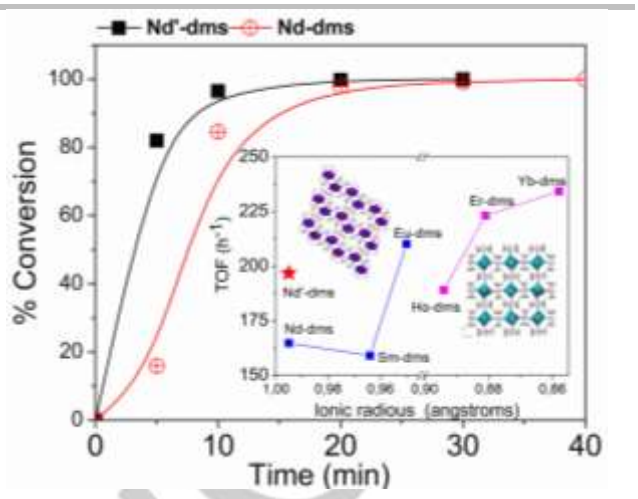

Figure 11: Kinetic profile of CSR with **Nd-dms** in comparison with **Nd'-dms** catalysts. Inset: TOF values for all the studied compounds (b).

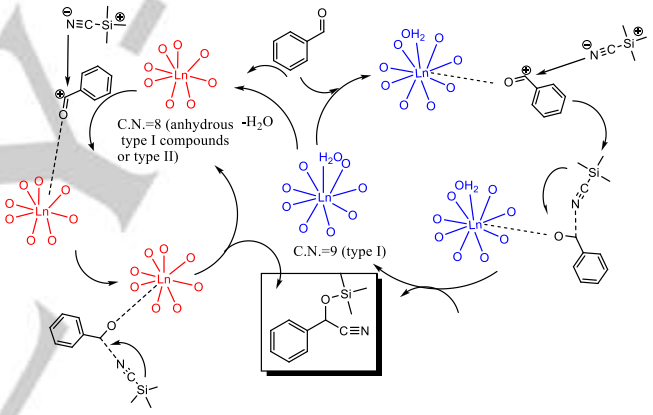

Figure 12: Mechanism of CSR of benzaldehyde employing **Ln-dms** compounds as catalysts.

Green metrics: On the basis of the new trends in currently chemistry, Anastas and Warner[44] introduced the concept of *Green Chemistry* with the purpose to overcome health and environmental problems derived from chemical industry by designing novel and eco-friendly chemical reactions leading to cleaner processes. Basically, the former concept emphasizes the efficient use of the starting materials (preferably recycled ones), minimizing waste generation as well as the use of toxic or hazardous reagents in the manufacture and application of chemicals. In this sense, a chemical process could be evaluated by determining the so called *green parameters*.[45] Thus, MI (mass intensity), AE (atomic economy),

CE (carbon efficiency) and RME (reaction mass efficiency) parameters are the measurements of sustainability to minimize the waste amount. The green metrics, ideally AE ≈ 100 %, MI ≈ 1, RME ≈ 100% and CE ≈ 100%, were calculated using the equations reported by Constable *et al.*[49] According to the results, the members of the **Ln-dms-2** series (see Table 3), exhibit the best values of green parameters in comparison with the **Ln-dms-1** and **Ln-psa**[10] ones. This trend is strongly associated with the catalytic performance of each group of Ln-compounds.

Table 3: Green parameters calculated for the CSR with **Ln-dms** as catalysts.

Ln-dms	MI	RME %
Nd-dms	8.0	64.8
Sm-dms	7.3	69.9
Eu-dms	7.1	73.0
Ho-dms	8.6	59.3
Yb-dms	6.9	74.5
Er-dms	7.3	71.0

Table 2: Summary of catalytic results of **Ln-dms** compounds in comparison with analogous phases using benzaldehyde as substrate.

Catalyst	Yield (%) (min)[a]	TOF (h^{-1})[b]	dimensionality	topology/point symbol	C.N.	Reference
Nd-dms	84.6 (40)	164.8	3D		9	**this study**
Eu-dms	95.8 (20)	159.1	3D	**bnn**/$4^6.6^4$	9	
Sm-dms	92.2(30)	210	3D		9	
Ho-dms	78.8 (30)	189.1	3D		8	
Yb-dms	97.6 (20)	234.2	3D	**fni**/$4^6.5.6^3$	8	**this study**
Er-dms	93 (20)	223.2	3D		8	
Eu-psa	69.9 (50)	83.9	2D		8,9****	
Sm-psa	79.9 (60)	95.9	2D		8,9****	
EuGd-psa	87.1 (60)	104.5	2D	**fes**/6^3	8,9****	10
Tb-psa	73.5 (30)	88.2	2D		8,9****	
Gd-psa	93.7 (20)	112.4	2D		8,9****	
EuTb-psa	85.9 (60)	103	2D		8,9****	
RPF-21-Pr	90.7 (240)	78.8	2D	**sql**	9	
RPF-22-Pr	54 (360)	10.2	2D	**SP2-(6,3)IIa**/$4^8.6^2$	8	
RPF-23-Pr	90.3 (360)	13.8	3D	*	8,9****	42a
RPF-21-La	93.2 (240)	71.2	2D	**sql**	9	
RPF-21-Nd	89.2 (240)	73	2D	**sql**	9	
RPF-18-Pr	77.8 (180)	6.48	2D		8	
RPF-18-La	85.7 (120)	9.38	2D	**SP2-(6,3)IIa**/$4^8.6^2$	8	46b
RPF-19-Nd	94.8 (120)	12.94	2D		9	
RPF-20-Nd	95 (180)	23.6	2D	**SP2-(6,3)IIa**/$4^8.6^2$	8	42d
Sc-MOF-1	84 (480)	2.5	2D	**kgd**/ $(4^3)2(4^6.6^6.8^3)$	6	
Sc-MOF-2	77.3 (510)	1.8	3D	**hcb**/6^3	6	11a
Sc-MOF-3	55 (420)	2.1	3D	**	7	
InPF-11	99 (40.2)	105	2D	1D chains	6	
InPF-12	99 (120)	284	1D	***	7	
InPF-13	93 (120)	298	1D	***	7	12a
InPF-14	99 (45)	105	3D	**la**	7	
InPF-15	80 (90)	265	3D	**SP1**/$4^2{\cdot}6$	6	

a. yield determined by GC-MS. b. TOF: mmol of substrate/mmol cat. 4-nodal net/$(3^2{\cdot}4^7{\cdot}5^4{\cdot}6^2)2$-$(3^2{\cdot}4^8{\cdot}5^3{\cdot}6^2)2(3^4{\cdot}4^{20}{\cdot}5^{14}{\cdot}6^{25}{\cdot}8^3)(4^6)2$. ** 1DSP 1-periodic net (4,4)(0,2)/$(4^2{\cdot}6)$. *** 4,6-c net (4-c) 2(6-c) 2-nodal net 4,6T40. **** There are two independent Ln centers into the structure.*

Conclusions

Two sets of metal–organic frameworks (MOFs) based on a flexible ligand and trivalent lanthanides were obtained solvothermally and fully characterized, to explore their optical properties at low temperature, magnetism and catalytic performance in relation to their structural features. In consonance with the 4f-4f transitions of the CF of each compound, the absorption spectra at low temperature to describe the "multisite nature" of the series were recorded. The magnetic properties **Nd-dms**, **Tb-dms**, **Dy-dms**, **Ho-dms** and **Er-dms** were studied in terms of magnetic susceptibility with the temperature, confirming a paramagnetic behaviour, except for **Nd-dms**, that shows an antiferromagnetic interaction at low temperature.

Moreover, the heterogeneous catalytic activity of the series was evaluated in one-pot cyanosilylation reaction with benzaldehyde as substrate. The metal acidity, the water content and microporosity were the factors taken into account to compare the results among the **Ln-dms-1** and **Ln-dms-2** compounds. Recyclability, structure conservation and catalytic efficiency were also evaluated showing a better performance taking into account the yield/time/TOF than the MOFs reported so far.

EXPERIMENTAL SECTION

Synthesis and characterizations: $[Ln_2(C_6H_8O_4)_3(H_2O)_2]$ **Ln-dms-1** (Ln=Nd, Pr, Sm, Eu) and $[Ln_2(C_6H_8O_4)_3]$ **Ln-dms-2** (Ln=Tb, Dy, Ho, Er, Yb) compounds were prepared hydrothermally employing the synthetic conditions previously reported by us[9a]: 1.5 mmoles of 2,3-dimethylsuccinic acid and 1 mmol of each lanthanide chloride were dissolved in 15 mL of distilled water. The pH value was adjusted to 3-4.5 with triethylamine or pyridine. The mixture was stirred for 30 minutes and then heated at 180 °C in a 120 mL Teflon-lined Parr bomb. After 72 h, the reaction was immediately cooled in cold water. Finally, the crystalline products were washed with mixtures a water/ethanol mixture and dried at room temperature (Figure 10). **Powder X-ray diffraction (PXRD)**: The X-ray diffraction patterns of all the compounds (Figure S11) were recorded using a Bruker D8-Advance Diffractometer with Cu-Kα radiation (λ_1= 1.54056 Å, λ_2= 1.54439 Å) operating at 40 kV and 40 mA and equipped with a LynxEye detector. MERCURY 2.0 program was used for molecular graphics for publication. CrystalExplorer program was used in order to study the microporosity of the compounds[46].

Optical studies: Optical absorption spectra were acquired with a Varian (model Cary 5E) spectrophotometer. MOF powders were dispersed in KBr (spectroscopic quality) and thin semitransparent pellets were produced by using static uniaxial pressure. Sample temperature was controlled by a close-cycled He cryostat.

Magnetic properties: Magnetic properties were measured on powder samples with a Quantum Design Versalab™ vibrating sample magnetometer. Measurements were performed between 50 and 300 K under the application of a magnetic field of 1 Tesla. The temperature dependence of the susceptibility was corrected using the corresponding Pascal's constants for the 2,3-dimethylsuccinate ligand.

Catalytic study: A typical procedure for cyanosilylation of benzaldehyde is as follows: Into a Pyrex-glass screw-cap vial, 10 mg (5 mmol %) of the catalyst were placed with 1 mL of dichloromethane (DCM) as solvent under room temperature. After that, 0.026 mL of benzaldehyde (BA) and 0.05 mL of trimethylsilyl cyanide (TMSC) in a 1:1.5 mmolar ratio were added. The reaction mixture was constantly stirred at 800 rpm under N_2 atmosphere. The conversion of BA and the product yield were periodically determined by gas chromatography (GC) analysis. When the reaction was completed, the catalyst was separated by centrifugation of the reaction mixture. All products were confirmed by comparison of their GC retention times and GC-MS analysis. GC analysis was performed using a Konik HRGC 400 B gas chromatograph-mass spectrometer equipped with a cross-linked 95% dimethyl-5% diphenylpolysiloxane (Teknokroma TRB-5MS) column of 30 m length.

Acknowledgements

G. E. G. acknowledges the doctoral and postdoctoral Consejo Nacional de Investigaciones Científicas y Técnicas (CONICET) fellowship. Also we thank to Dr. Carlos Zaldo, Concepción Cascales, Marta Iglesias, and María A. Monge from Instituto de Ciencia de Materiales de Madrid for their contributions of the present work. We also thank to Dr. Claudio Borsarelli from UNSE for his help in obtaining the diffuse reflectance measurements. G. E. G., G. E. N. and G. J. A. A. S. I. are members of CIC-CONICET. This work was supported by the CONICET (PIP CONICET 112-201101-00912), ANPCyT PICT-2012-1994 and UNSL (PROICO 2-1612).

.

Keywords: Lanthanides • 2,3-dimethylsuccinate • Metal-Organic Frameworks • Crystal Field • Catalysis

FULL PAPER

An in depth analysis of the 4f-4f optical (high resolution absorptions at low temperature), magnetic and catalytic properties of a set of 3D lanthanide MOFs based on 2,3-dimethylsuccinate (**Ln-dms 1** and **2**) was made in correlation with their structural features. According with the catalytic performances in cyanosylilation of benzaldehyde reaction, **Ln-dms-2** structures exhibit promising results as acids solid catalysts with high conversions in short times.

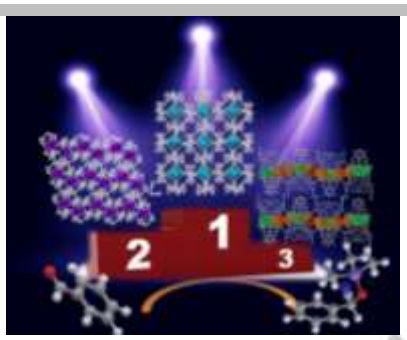

MOFs optics, magnetism and catalysis

Germán E. Gomez, Elena V. Brusau, Joaquín Sacanell, Galo J. A. A. Soler Illia and Griselda E. Narda**

An insight into the metal content-structure-property relationship in lanthanide metal-organic frameworks: optical studies, magnetism and catalytic performance

References

[1] A. Corma, H. García, F. X. Llabrés i Xamena, *Chem. Rev*. **2010**, *110,* 4606-4655.

[2] a) R. Custelcean, B. A. Moyer, *Eur. J. Inorg. Chem.* **2007**, *10*, 1321-1340; b) J. R. Li, J. Sculley, H. C. Zhou, *Chem. Rev.* **2012**, *112*, 869-932.

[3] a) P. Horcajada, T. Chalati, C. Serre, B. Gillet, C. Sebrie, T. Baati, J. F. Eubank, D. Heurtaux, P. Clayette, C. Kreuz, J. S. Chang, Y. K. Hwang, V. Marsaud, P. N. Bories, L. Cynober, S. Gil, G. Férey, P. Couvreur, R. Gref, *Nat. Mat*. **2010**, *9*, 172–178; b) V. Agostoni, T. Chalati, P. Horcajada, H. Willaime, R. Anand, N. Semiramoth, T. Baati, S. Hall, G. Maurin, H. Chacun, K. Bouchemal, C. Martineau, F. Taulelle, P. Couvreur, C. Rogez-Kreuz, P. Clayette, S. Monti, C. Serre, R. Gref, *Adv Healthcare Mater*., **2013**; *2* (12), 1630-1637; c) C. Tamames-Tabar, D. Cunha, E. Imbuluzqueta, F. Ragon, C. Serre, M. J. Blanco-Prieto, P. Horcajada, *J. Mater. Chem. B,* **2014**, *2*, 262-271.

[4] a) J. Heinea, K. Müller-Buschbaum , *Chem. Soc. Rev*., **2013**, *42*, 9232-9242; b) W. P. Lustig, S. Mukherjee, N. D. Rudd, A. V. Desai, J. Li, S. K. Ghosh, *Chem. Soc. Rev*., **2017**, *46*, 3242-3285.

[5] a) J. M. Frost, K. L. M. Harrimana, M. Murugesu, *Chem. Sci.*, **2016**, *7*, 2470-2491; b) D. N. Woodruff, R. E. P. Winpenny, R. A. Layfield, *Chem. Rev* , **2013**, *113*(7), 5110-5148.

[6] B. Li, H.-M- Wen, Y. Cui, W. Zhou, G. Qian, B. Chen, *Adv. Mater.* **2016**, *28*(40), 8819-8860.

[7] R. F. D'Vries, G. E. Gomez, D. F. Lionello, M. C. Fuertes, G. J. A. A. Soler-Illia, J. Ellena, *RSC Adv*., **2016**, *6 (111)*, 110171-110181.

[8] G. E. Gomez, R. F. D'vries, D. F. Lionello, L. M. Aguirre-Díaz, M. Spinosa, C. S. Costa, M. C. Fuertes, R. A. Pizarro, A. M. Kaczmarek, J. Ellena, L. Rozes, M. Iglesias, R. Van Deun, C. Sanchez, M. A. Monge, G. J. A. A. Soler-Illia, *Dalton Trans*., **2018**, *47*, 1808-1818.

[9] a) G. E. Gomez, M. C. Bernini, E. V. Brusau, G. E. Narda, W. A. Massad, A. Labrador, *Cryst. Growth Des.*, **2013**, *13*, 5249-5260; b) G. E. Gomez, M. C. Bernini, E. V. Brusau, G. E. Narda, D. Vega, A. M. Kaczmarek, R. Van Deun, M. Nazzarro, *Dalton Trans*., **2015**, *44*, 3417-3429; c) R. F. D'Vries, G. E. Gomez, J. H. Hodak, G. J. A. A. Soler-Illia, J. Ellena, *Dalton Trans*., **2016**, *45*, 646-656.

[10] G. E. Gomez, A. M. Kaczmarek, R. Van Deun, E. V. Brusau, G. E. Narda, D. Vega, M. Iglesias, E. Gutierrez-Puebla, M. Ángeles Monge, *Eur. J. Inorg. Chem*., **2016**, 1577-1588.

[11] a) R. F. D'Vries, V. A. de la Peña-O'Shea, N. Snejko, M. Iglesias, E. Gutiérrez-Puebla, M. A. Monge, *J. Am. Chem. Soc.*, **2013**, *135*, 5782-5792; b) M. C. Bernini, V. A. de la Peña-O'Shea, M. Iglesias, N. Snejko, E. Gutierrez-Puebla, E. V. Brusau, G. E. Narda, F. Illas, M. A. Monge, *Inorg. Chem.*, **2010**, *49*, 5063-5071.

[12] a) L. M. Aguirre-Díaz, D. Reinares-Fisac, M. Iglesias, E. Gutiérrez-Puebla, F. Gándara, N. Snejko, M. A. Monge, *Coord. Chem. Rev*., **2017**, *335*, 1-27.; b) L. M. Aguirre-Díaz, M. Iglesias, N. Snejko, E. Gutiérrez-Puebla, M. A. Monge, *RSC Adv.*, **2015**, *5*, 7058-7065.

[13] R. F. D'Vries, Susana Álvarez-García, Natalia Snejko, Luisa E. Bausá, Enrique Gutiérrez-Puebla, Alicia de Andrés, M. A. Monge, *J. Mat. Chem. C*, **2013**, *1(39)*, 6316-6324.

[14]a) G. E. Gomez, E. V. Brusau, A. M. Kaczmarek, C. Mellot-Draznieks, J. Sacanell, G. Rousse, R. Van Deun, C. Sanchez, G. E. Narda, G. J. A. A. Soler Illia, *Eur. J. Inorg. Chem*., **2017**, *2017 (17)*, 2321-2331; b) A. A. Godoy, G. E. Gomez, A. M. Kaczmarek, R. Van Deun, O. J. Furlong, F. Gándara, M. A. Monge, M. C. Bernini, G. E. Narda, *J. Mater. Chem. C*, **2017**, *5*, 12409-12421.

[15] a) M. C. Bernini, E. V. Brusau, G. E. Narda, G. E. Echeverria, C. G. Pozzi, G. Punte, Christian W. Lehmann, *Eur. J. Inorg. Chem.*, **2007**, *2007(5)*, 684-693; b) M. C. Bernini, A. E. Platero Prats, R. Saez Puche, J. Romero de Paz, M. A. Monge, *CrystEngComm*., **2012**, *14 (17)*, 5493-5504.

[16] a) C. Janiak, *Dalton Trans*, **2003**, 2781-2804; b) S. M. Krishnan, R. M. Supkowski, R. L. LaDuca, *J. Mol. Struct.*, **2008**, *891*, 423–428.

[17] a) D.Ghoshal, A. Kumar Ghosh, G. Mostafa,; J. Ribas, N. Ray Chaudhuri, *Inorg. Chim. Acta*, **2007**, *360* (5), 1771-1775; b) N. Guillou, C. Livage, G. Ferey, *Eur. J. Inorg. Chem*., **2006**, *24*, 4963-4978; c) N. Guillou, C. Livage, W. Van Beek, M. Nogues, G. Férey, *Angew. Chem., Int. Ed*., **2003**, *42* (6), 644-647; d) P. M. Forster, A. K. Cheetham, *Angew. Chem., Int. Ed*., **2002**, *41* (3), 457-459; e) R. Vaidhyanathan, S. Natarajan, C. N. R. Rao, *Inorg. Chem*., **2002**, *41* (20), 5226-5234; f) A. R. Burbank, M. C. O'Sullivan, N. Guillou, C. Livage, G. Férey, N. Stock, A. K. Cheetham, *Solid State Sci.*, **2005**, *7* (12), 1549-1555; g) P. M. Forster, N. Stock, A. K. Cheetham, *Angew. Chem., Int. Ed*., **2005**, *44* (46), 7608-7611; h) P. M. Forster, A. R. Burbank, C. Livage, G. Férey, A. K Cheetham,. *Chem. Commun*., **2004**, *10* (4), 368-369.

[18] a) F. Serpaggi, G. Férey, *Microporous Mesoporous Mater*., **1999**, *32,* 311-318; b) A. Seguatni, M. Fakhfakh, M. J. Vauley, N. Jouini, *J. Solid. State Chem*., **2004**, *177,* 3402-3410; c) G.-H. Cui, J.-R. Li, R.-H. Zhang, X.-H. Bu, *J. Mol. Struct.,* **2005**, *740,* 187-191; d) X. J. Zhang, Y. H. Xing, J. Han, *J. Coord. Chem*., **2008**, *61,* 651-660.

[19] J.-Y. Kim, A. J. Norquist, D. O'Hare, *Dalton Trans*., **2003**, 2813-2814.

[20] R. F. D'Vries, M. Iglesias, N. Snejko, S. Alvarez-Garcia, E. Gutiérrez-Puebla, M. A. Monge, *J. Mater. Chem*., **2012**, *22*, 1191-1198

[21] M. C Bernini,. E. V. Brusau, G. E. Narda, G. E. Echeverria, C. G. Pozzi, G. Punte, C. W. Lehmann, *Eur. J. Inorg. Chem*., **2007**, 684-693

[22] M. C. Bernini, F. Gándara, M. Iglesias, N. Snejko, E. Gutiérrez-Puebla, E. V. Brusau, G. E. Narda, M. A. Monge, *Chem. Eur. J.*, **2009**, *15*, 4896-4905.

[23] P. J. Saines, M. Steinmann, J.-C. Tan, H. H.-M. Yeung, A. K. Cheetham, *CrystEngComm*, **2013**, *15*, 100-110.

[24] F. Gándara, A. de Andrés, B. Gómez-Lor, E. Gutiérrez-Puebla, M. Iglesias, M. A. Monge, D. M. Proserpio, N. Snejko, *Cryst. Growth Des.*, **2008**, *8(2)*, 378-380.

[25] F. Gándara, E. Gutiérrez-Puebla, M. Iglesias, D. M. Proserpio, N. Snejko, M. A. Monge, *Chem. Mater.,* **2009**, *21(4)*, 655-661.

[26] a) M. A. Lacour, N. J. Rhaier, M. Taillefer, *Chem.Eur. J.* **2011**, *17(44)*, 12276-12279; b) R. J. H. Gregory, *Chem. Rev*. **1999**, *99(12)*, 3649-3682; c) J. –M. Brunel, I. P. Holmes, *Angew. Chem., Int. Ed*. **2004**, *43(21)*, 2752-2778.

[27] a) B. Y. Park, K. Y. Ryu, J. H. Park, S. G. Lee, *Green Chem*., **2009**, *11*, 946-948; b) N. Kurono, M. Yamaguchi, K. Suzuki, T. Ohkuma, *J. Org. Chem*., **2005**, *70(16)*, 6530-6532; c) P. Saravanan, R. Vijaya Anand, V. K. Singh, *Tetrahedron Lett.*, **1998**, *39(22)*, 3823-3824; d) Y. Ogasawara, S. Uchida, K. Yamaguchi, N. Mizuno, *Chem.Eur. J.,* **2009**, *15(17)*, 4343-4349; (e) A. Procopio, G. Das, M. Nardi, M. Oliverio, L. A. Pasqua, *ChemSusChem.,* **2008**, *1(11)*, 916-919; f) K. Iwanami, J. C. Choi, B. Lu, T. Sakakura, H. Yasuda, *Chem. Commun*., **2008**, 1002-1004. g) W. K. Cho, J. K. Lee, S. M. Kang, Y. S. Chi, H. S. Lee, I. S. Chio, *Chem.Eur. J.,* **2007**, *13(22)*, 6351-6358; h) S. Huh, H. T. Chen,J. W. Wiench, M. Pruski, V. S. Y. Lin, *Angew. Chem., Int. Ed.* **2005**, *44(12)*, 1826-1830; i) K. Yamaguchi, T. Imago, Y. Ogasawara, J. Kasai, M. Kotani, N. Mizuno, *.Adv. Synth. Catal*., **2006**, *348(12-13)*, 1516-1520; j) B. Karimi, L. A. Ma'Mani, *Org. Lett*., **2004**, *6(26)*, 4813-4815; k) K. Higuchi, M. Onaka, Y. Izumi, *Bull.Chem. Soc. Jpn*., **1993**, *66(7)*, 2016-2032.

[28] L. D. Carlos, R. A. S. Ferreira, V. de Zea Bermúdez, S. J. L. Ribeiro, *Adv. Mater*., **2009**, *21*, 509-534.

[29] a) C. Cascales, R. Balda, J. M. Fernández-Navarro, *J. Opt. Express*, **2005**, *13*, 2141-2152. b) C. Cascales, C. Zaldo, R. Sáez Puche, *Chem. Mater*. **2005**, 17, 2052-2058. c) C. Cascales, R. Balda, J. M. Fernández-Navarro, *J. Non- Cryst. Solids*, **2006**, *352*, 2448-2451.

[30] S. Torelli, D. Imbert, M. Cantuel, G. Bernardinelli, S. Delahaye, A. Hauser, J. C. Bünzli, C. Piguet, *Chem. Eur. J.*, **2005**, *11*, 3228-3242.

[31] a) X. Guo, G. Zhu, Q. Fang, M. Xue, G. Tian, J. Sun, X. Li, S. Qiu, *Inorg. Chem.*, **2005**, *44*, 3850-3855. b) R. X. Yan, Y. D. Li, *Adv. Funct. Mater.*, **2005**, *15*, 763-770. c) H. W. Song, L. X. Lu, L. M. Yang, S. Z. Lu, *J. Nanosci. Nanotechnol.* **2005**, *5*, 1519-1531. d) A. Q. Le Quang, J. Zyss, I. Ledoux, V. G. Truong, A. M. Jurdyc, B. Jacquier, D. H. Le, A. Gibaud, *Chem. Phys*., **2005**, *318*, 33-43.

[32] a) J. C. G. Bünzli, S. Comby, A.-S. Chauvin, C. D. V. Vandevyver, *J. Rare Earths*, **2007**, *25*, 257-274; b) K. Binnemans, *Chem. Rev.*, **2009**, *109*, 4283-4374.

[33] M. H. V. Werts, *Sci. Pro*. **2005**, *88*, 101-131.

[34] a) K. Kuriki, Y. Koike, Y. Okamoto, *Chem. Rev*., **2002**, *102*, 2347-2356; b) A. Polman, F. C. J. M. van Veggel, *J. Opt. Soc. Am. B.*, **2004**, *21*, 871-892.

[35] X. Han, E. Castellano-Hernández, J. Hernández-Rueda, J. Solís, C. Zaldo, *Opt. Express*., **2014**, *22(20)*, 24111-24116.

[36] a) C. D. S. Brites, P. P. Lima, N. J. O. Silva, A. Millán, V. S. Amaral, F. Palacio, L. D. Carlos, *Nanoscale*, **2012**, *4*, 4799-4829. b) Y. Cui, H. Xu, Y. Yue, Z. Guo, J. Yu, Z. Chen, J. Gao, Y. Yang, V. Qian, B. A. Chen, *J. Am. Chem. Soc.*, **2012**, *134*, 3979-3982; c) X. T. Rao, T. Song, J. K. Gao, Y. J. Cui ,Y. Yang, C. D. Wu, B. L. Chen, G. D. Qian, *J. Am. Chem. Soc.*, **2013**, *135*, 15559-15564; d) Y. Cui, W. Zou, R. Song, J. Yu, W. Zhang, Y. Yang, G. Qian, *Chem. Commun.*, **2014**, *50*, 719-721; e) Y. Cui, R. Song, J. Yu, M. Liu, Z. Wang, C. Xu, Y. Yang, Z. Wang, B. Chen, G. Qian, *Adv. Mater*., **2015**, *27(8)*, 1420-1425. f) A. Cadiau, C. D. S. Brites, P. M. F. J. Costa, R. A. S. Ferreira, J. Rocha, L. D. Carlos, *ACS Nano*., **2013**, *7*, 7213-7218; g) Z. Wang, D. Ananias, A. Carné-Sánchez, C. D. S. Brites, I. Imaz, D. Maspoch, J. Rocha, L. D. Carlos, *Adv. Func. Mater*., **2015**, *25(19)*, 2824-2830. h) M. Ren, C. D. S. Brites, S.-S. Bao, R. A. S. Ferreira, L.-M. Zheng, L. D. Carlos, *J. Mater. Chem. C*, **2015**, *3*, 8480-8484. i) K. Miyata, Y. Konno,T. Nakanishi, A. Kobayashi, M. Kato, K. Fushimi, Y. Hasegawa, *Angew. Chem. Int. Edit.*, **2013**, *52*, 6413-6416; j) Y. Zhou, B. Yan, F. Lei, *Chem. Commun.*, **2014**, *50*, 15235-15238; k) S.-N. Zhao, L.-J. Li, X.-Z. Song, M. Zhu, Z.-M. Hao, X. Meng, L.-L. Wu, J. Feng, S.-Y. Song, C. Wang, H.-J. Zhang, *Adv. Funct. Mater.*, **2015**, *25*, 1463–1469; l) Y. Wei, R. Sa, K. Wu, *Dalton Trans.*, **2015**, *44*, 3067-3074; m) X. Shen, Y. Lu, B. Yan, *Eur. J. Inorg. Chem.*, **2015**, *6*, 916-

919; n) Y. Zhou, B. Yan, *J. Mater. Chem. C*, **2015**, *3*, 9353-9358. o) X. Liu, S. Akerboom, M. de Jong, I. Mutikainen, S. Tanase, A. Meijerink, E. Bouwman, *Inorg. Chem.*, **2015**, *54(23)*, 11323-11329.

[37] J. Marling, *IEEE J. Sel. Top. Quantum Electron*., **1978**, *14*, 56-62.

[38] C. K. Jørgensen, B. R. Judd, *Mol. Phys*. **1964**, 8, 281-290

[39] E. Antic-Fidancev, *J. Alloys Comp*. **2000**, *300*, 2-10.

[40] C. Benelli, D. Gatteschi, *Chem. Rev.*, **2002**,*102*, 2369-2387.

[41] a) Kobayashi, S.; Sugiura, M.; Kitagawa, H.; Lam, W. W. L. *Chem. Rev*., (**2002**), *102*, 2227-2302. b) Kobayashi, S.; Mori, Y.; Yamashita, Y. In Comprehensive Coordination Chemistry II; McCleverty, J. A., Meyer, T. J., Eds.; Pergamon: Oxford, **2003**.

[42] a) R. F. D'Vries, V. A. de la Peña-O'Shea, N. Snejko, M. Iglesias, E. Gutiérrez-Puebla, M. A. Monge. *Cryst. Growth Des*., **2012**, *12(11)*, 5535-5545; b) R. F. D'Vries, M. Iglesias, N. Snejko, E. Gutiérrez-Puebla, M. A. Monge. *Inorg. Chem*., **2012**, *51*, 11349-11355; c) L. M. Aguirre-Díaz, M. Iglesias, N. Snejko, E. Gutiérrez-Puebla, M. Ángeles Monge. *CrystEngComm*, **2013**, *15*, 9562–9571; d) R. F. D'Vries, N. Snejko, M. Iglesias, E. Gutiérrez-Puebla, M. A. Monge. *Cryst. Growth Des*., **2014**, *14*, 2516-2521.

[43] S. Kozuch, J. M. L. Martin, *ACS Catal.*, **2012**, *2*, 2787–2794.

[44]P. T. Anastas, J. C. Warner, *Green Chemistry: Theory and Practice*, Oxford University Press, New York, 1998.

[45]D. J. C. Constable, A. D. Curzons, V. L. Cunningham, *Green Chem*., **2002**, *4*, 521-527.

[46] M. J. Turner, J. J. McKinnon, D. Jayatilaka, M. A. Spackman, *CrystEngComm*, **2011**, *13*, 1804-1813.